

*Supporting information for*

# 2D Covalent Organic Frameworks with Carbazole-embedded Frameworks Facilitate Photocatalytic and electrocatalytic Processes

Yuchen Xiao<sup>1,2,3</sup>, Shanyue Wei<sup>1,2,4</sup>, Xiaowei Wu<sup>1,2,\*</sup> and Can-Zhong Lu<sup>1,2,3,\*</sup>

<sup>1</sup> State Key Laboratory of Structural Chemistry, Fujian Institute of Research on the Structure of Matter, Chinese Academy of Sciences, Fuzhou 350002, China.

<sup>2</sup>Xiamen Key Laboratory of Rare Earth Photoelectric Functional Materials, Xiamen Institute of Rare Earth Materials, Haixi Institutes, Chinese Academy of Sciences, Xiamen, 361021, China.

<sup>3</sup>School of Physical Science and Technology, ShanghaiTech University, Shanghai, 201210, China.

<sup>4</sup>Engineering Research Center of Environment-Friendly Function Materials, Ministry of Education, College of Materials Science & Engineering, Huaqiao University, Xiamen 361021, China.

Email: xmwuxiaowei@fjirsm.ac.cn; czlu@fjirsm.ac.cn

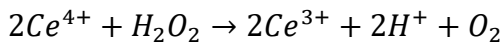
## 1. Methods

**Crystal structure modeling:** Structural modeling of COFs was generated using the Materials Studio program (ver2019), the lattice model was geometrically optimized using force-field based method (Forcite, UFF, Ewald summations, Q<sub>eq</sub>). Pawley fitting was conducted by using the Reflex module.

**Density-functional theory simulation:** The electrostatic potential and molecular orbital of COFs were calculated using DFT based on the Materials Studios (MS) software. Considering the limitation of computing resources, the model is established by using FCTD coupled with two amino monomers via imine linkage. GGA-BLYP function of DMol3 module was used for carrying out structural optimization and calculating electrostatic potential and molecular orbital. The electronic energy was considered self-consistent when the energy change was smaller than 10<sup>-5</sup> eV. A geometry optimization was considered convergent when the force change was smaller than 0.02 eV/Å.

**H<sub>2</sub>O<sub>2</sub> quantification:** The H<sub>2</sub>O<sub>2</sub> concentration was measured by traditional cerium sulfate Ce(SO<sub>4</sub>)<sub>2</sub> titration method based on the mechanism that a yellow solution of

$\text{Ce}^{4+}$  would be reduced by  $\text{H}_2\text{O}_2$  to colorless  $\text{Ce}^{3+}$ .

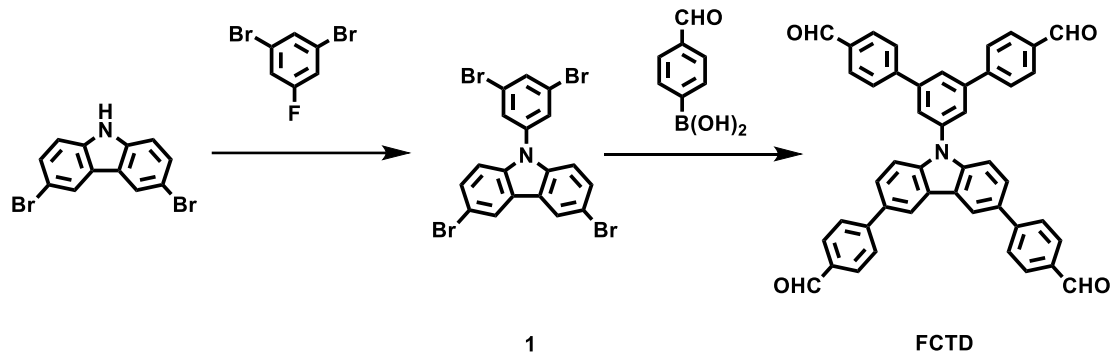


Therefore, the concentration of  $\text{H}_2\text{O}_2$  (M) can be determined by the following equation:  $M(\text{H}_2\text{O}_2) = \frac{1}{2}\Delta M(\text{Ce}^{4+})$ .

Typically, the yellow transparent  $\text{Ce}(\text{SO}_4)_2$  solution (1 mM) was prepared by dissolving 33.2 mg  $\text{Ce}(\text{SO}_4)_2$  in 100 ml 0.5 M sulfuric acid solution. Then the collected electrolyte (400  $\mu\text{l}$ ) was titrated into 3 mL  $\text{Ce}(\text{SO}_4)_2$  solution (1 mM) and shaking the mixed solution for two minutes. As a counterpart, the 400  $\mu\text{L}$  0.1 M KOH solution were titrated into 3 mL  $\text{Ce}(\text{SO}_4)_2$  solution (1 mM) to obtain the mixed solution unreacted. Based on the linear relationship between the signal intensity of ultraviolet-visible spectroscopy (at around 319 nm) and  $\text{Ce}^{4+}$  concentration. The concentration of  $\text{Ce}^{4+}$  before and after the reaction can be measured by ultraviolet-visible spectroscopy. Therefore, the  $\text{H}_2\text{O}_2$  concentrations of the samples could be obtained.

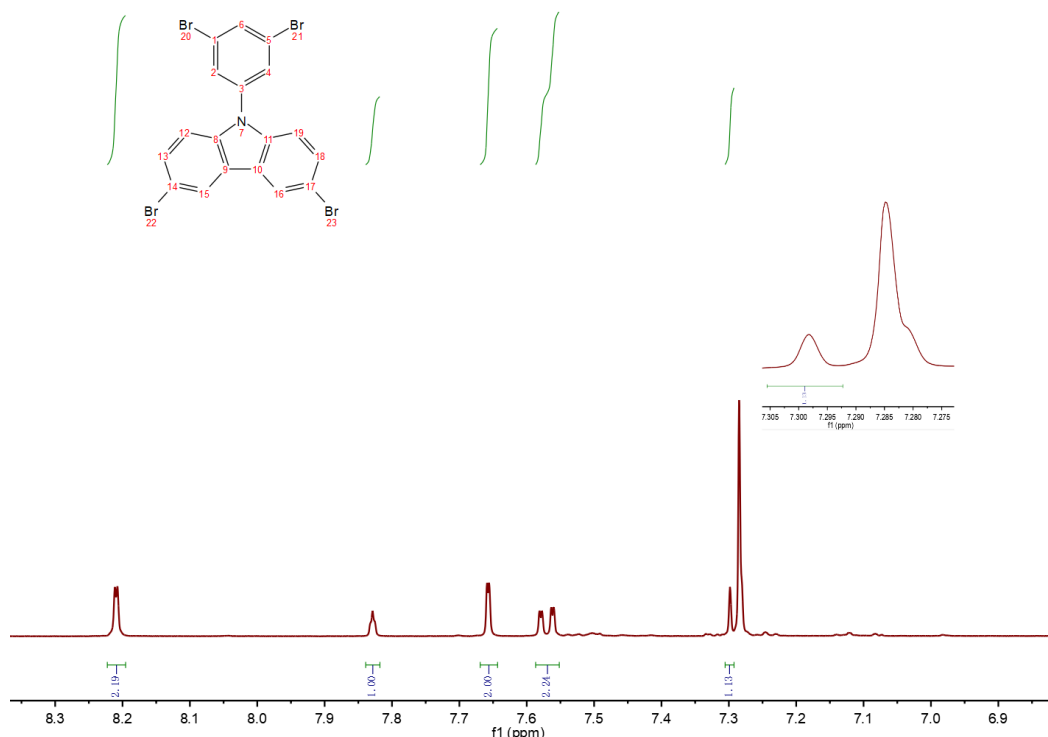
## 2. Synthesis procedures

### 5'-(3,6-bis(4-formylphenyl)-9H-carbazol-9-yl)-[1,1':3',1"-terphenyl]-4,4"-dicarba ldehyde (FCTD)

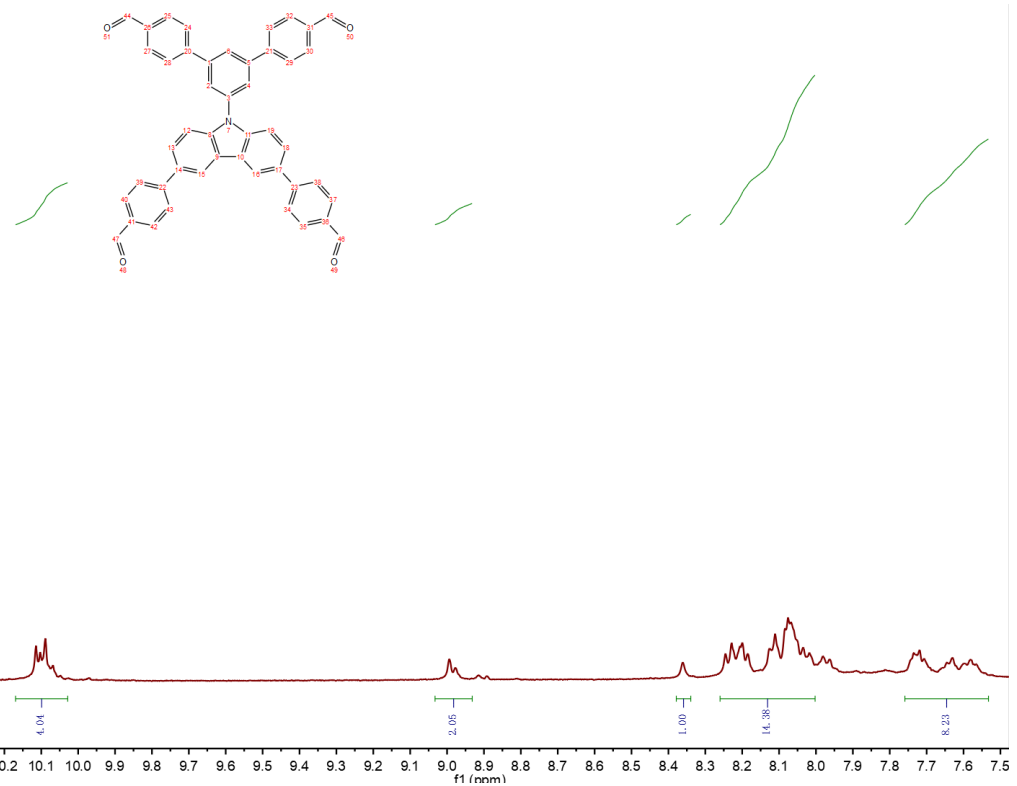


975 mg (3 mmol, 1 eq.) 3,6-dibromo-9H-carbazole, 1.52 mL (3048 mg, 12 mmol, 4 eq.) 1,3-dibromo-5-fluorobenzene, 3910 mg (12 mmol, 4 eq.)  $\text{Cs}_2\text{CO}_3$  and 30 mL N, N-Dimethylformamide were weighed and packed in 100 mL round-bottom flask. The reaction was stirred at 150°C for 24h in air atmosphere. After cooling to room temperature, water is added to precipitate the solid. Filter and wash solids with salt

water and ethyl acetate in turn, drying in vacuum to give a grey powder of **1** (yield: 85%).  $^1\text{H}$  NMR (500 MHz, Chloroform-d)  $\delta$  8.21 (d, 2H), 7.83 (t, 1H), 7.66 (d, 2H), 7.57 (dd, 2H), 7.29 (d, 2H).



280 mg (0.5 mmol, 1 eq.) **1**, 375 mg (2.5 mmol, 5 eq.) 4-formylphenylboronic acid, 553 mg (4 mmol, 8 eq.)  $\text{K}_2\text{CO}_3$  and 11.6 mg (0.01 mmol, 0.02 eq.)  $\text{Pd}(\text{PPh}_3)_4$  were weighed and packed in 120 mL pressure bottle and adding 15 mL 1,4-dioxane and 3 mL  $\text{H}_2\text{O}$  as solvent. The mixture was vacuumed and filled with inert gas three times and stirred at 120 °C for 24 h. After cooling to room temperature, the mixture was filtrated followed by rinsing with water and alcohol, and drying in vacuum to give 284 mg yellow powder of 5'-(3,6-bis(4-formylphenyl)-9H-carbazol-9-yl)-[1,1':3',1"-terphenyl]-4,4"-dicarbaldehyde (yield: 86%).  $^1\text{H}$  NMR (500 MHz,  $\text{DMSO-d}_6$ )  $\delta$  10.13 – 10.06 (m, 4H), 9.02 – 8.88 (m, 2H), 8.38 – 8.34 (s, 1H), 8.26 – 7.95 (m, 14H), 7.76 – 7.54 (m, 8H).



### FCTD-TAPy

**FCTD** (19.8 mg, 0.03 mmol) and **TAPy** (17.0 mg, 0.03 mmol) were added into a 10 mL Pyrex tube; then, a mixture of N,N-dimethylacetamide (DMAC, 1.0 mL), *n*-butanol (n-BuOH, 1.0 mL), and acetic acid (aq 6 M, 0.2 mL) was added into this Pyrex tube. The Pyrex tube was sealed after being evacuated under vacuum for three pump–thaw cycles in a liquid nitrogen bath. After that, the sealed Pyrex tube was placed in a vacuum oven at 120 °C for 3 days. The solid was isolated by centrifugation, washed with ethyl acetate, and further purified by Soxhlet extraction with tetrahydrofuran, methanol, and trichloromethane. The sample was then transferred to a vacuum chamber and evacuated to 20 mTorr at 50 °C for 24 h, yielding COFs as yellow powders (yield: 33.2 mg, 90.02%).

### FCTD-TAET

**FCTD** (19.8 mg, 0.03 mmol) and **TAET** (11.8 mg, 0.03 mmol) were added into a 10 mL Pyrex tube; then, a mixture of N,N-dimethylacetamide (DMAC, 1.0 mL), mesitylene(Mes, 1.0 mL), and acetic acid (aq 6 M, 0.2 mL) was added into this Pyrex tube. The Pyrex tube was sealed after being evacuated under vacuum for three pump–thaw cycles in a liquid nitrogen bath. After that, the sealed Pyrex tube was placed in a

vacuum oven at 120 °C for 3 days. The solid was isolated by centrifugation, washed with ethyl acetate, and further purified by Soxhlet extraction with tetrahydrofuran, methanol, and trichloromethane. The sample was then transferred to a vacuum chamber and evacuated to 20 mTorr at 50 °C for 24 h, yielding COFs as yellow powders (yield: 30.0 mg, 94.64%).

### FCTD-TABT

**FCTD** (19.8 mg, 0.03 mmol) and **TABT** (19.6 mg, 0.03 mmol) were added into a 10 mL Pyrex tube; then, a mixture of o-dichlorobenzene (o-DCB, 1.0 mL), n-butanol (n-BuOH, 1.0 mL), and acetic acid (aq 6 M, 0.2 mL) was added into this Pyrex tube. The Pyrex tube was sealed after being evacuated under vacuum for three pump–thaw cycles in a liquid nitrogen bath. After that, the sealed Pyrex tube was placed in a vacuum oven at 120 °C for 3 days. The solid was isolated by centrifugation, washed with ethyl acetate, and further purified by Soxhlet extraction with tetrahydrofuran, methanol, and trichloromethane. The sample was then transferred to a vacuum chamber and evacuated to 20 mTorr at 50 °C for 24 h, yielding COFs as yellow powders (yield: 29.7 mg, 75.38%).

## 3. Experimental data

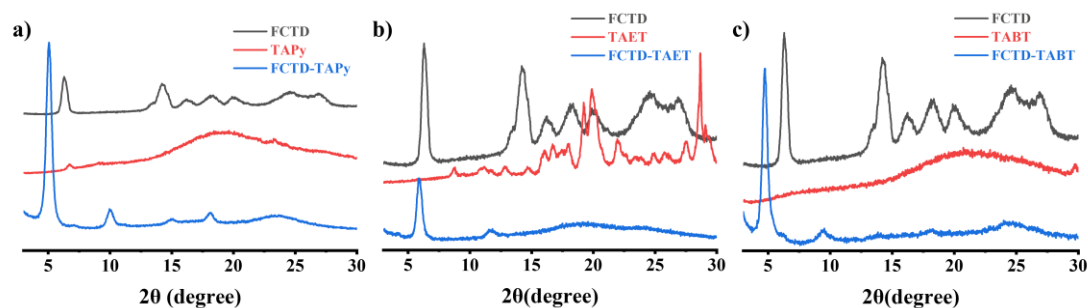


**Figure S1.** PXRD of (a) FCTD-TAPy, (b) FCTD-TAET, and (c) FCTD-TABT

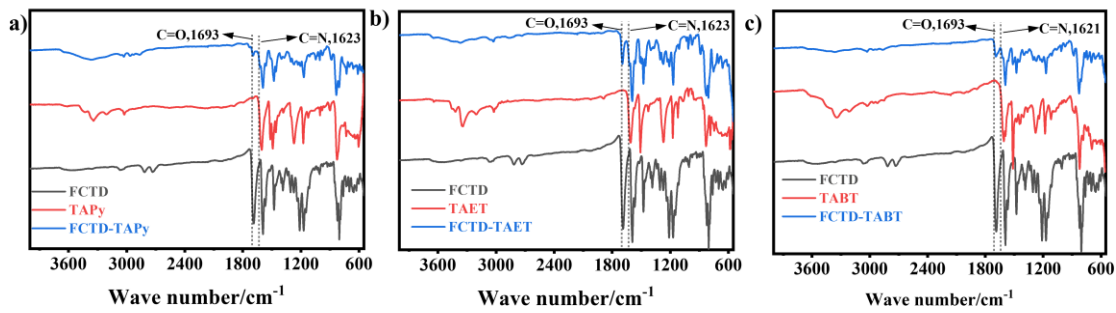


**Figure S2.** FT-IR spectra of (a) FCTD-TAPy, (b) FCTD-TAET, and (c) FCTD-TABT

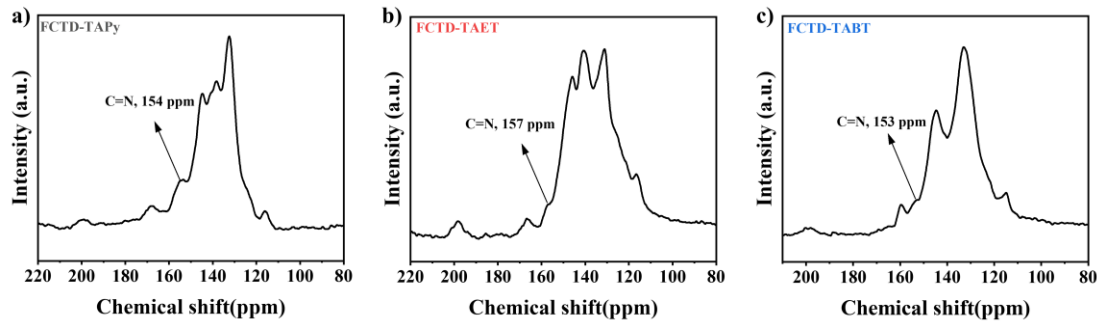


**Figure S3.**  $^{13}\text{C}$  CP/MAS NMR spectra of (a) FCTD-TAPy, (b) FCTD-TAET, and (c) FCTD-TABT

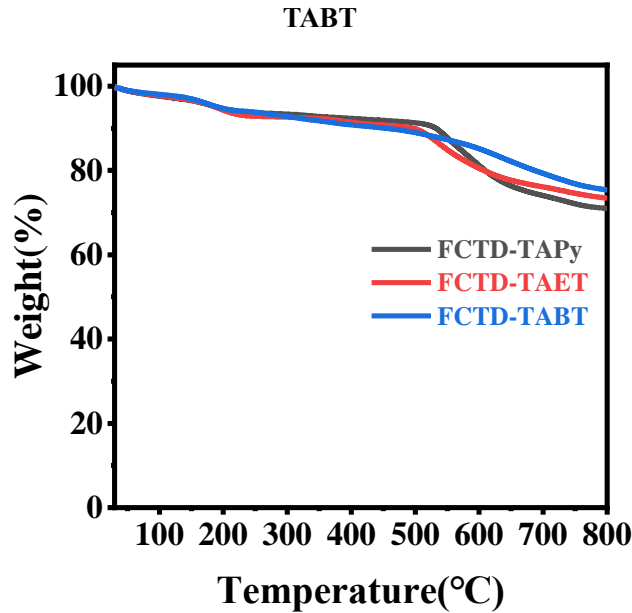


**Figure S4.** Thermogravimetric curves of FCTD-TAPy, FCTD-TAET, and FCTD-TABT under argon atmosphere

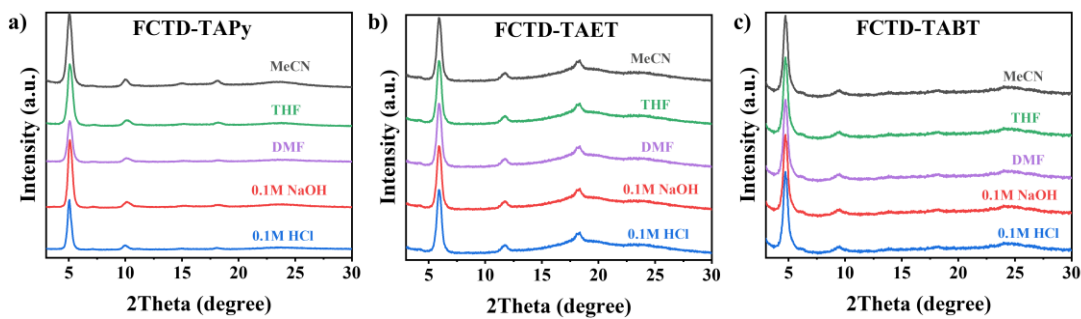


**Figure S5.** The chemical stabilities for (a) FCTD-TAPy, (b) FCTD-TAET, and (c) FCTD-TABT under different solvents.

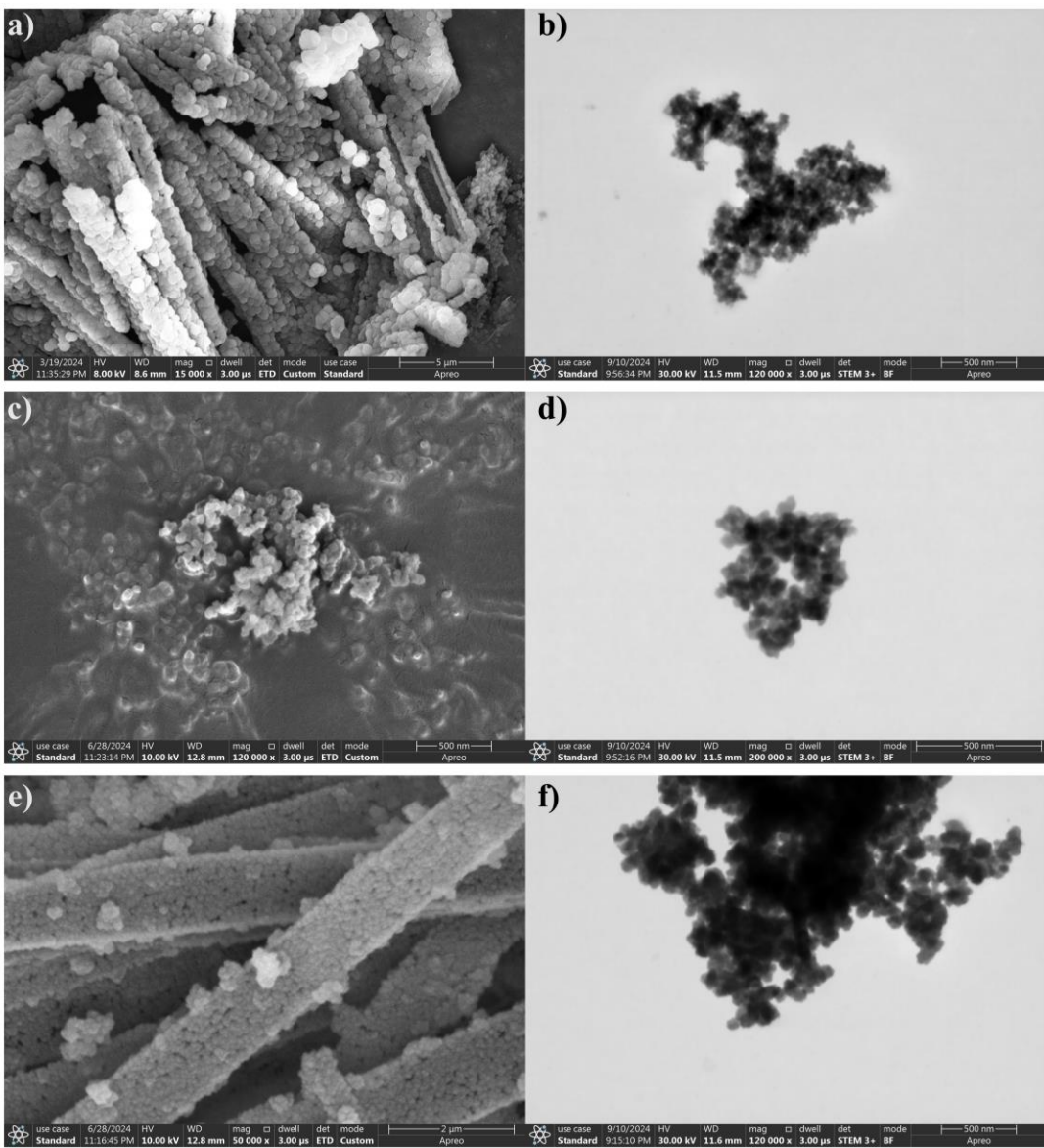


**Figure S6.** The SEM and TEM images of (a-b) FCTD-TAPy, (c-d) FCTD-TAET, and (e-f) FCTD-TABT

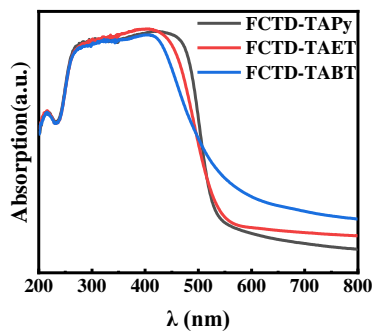


**Figure S7.** UV/visible absorption spectra of the FCTD-TAPy, FCTD-TAET, and FCTD-TABT

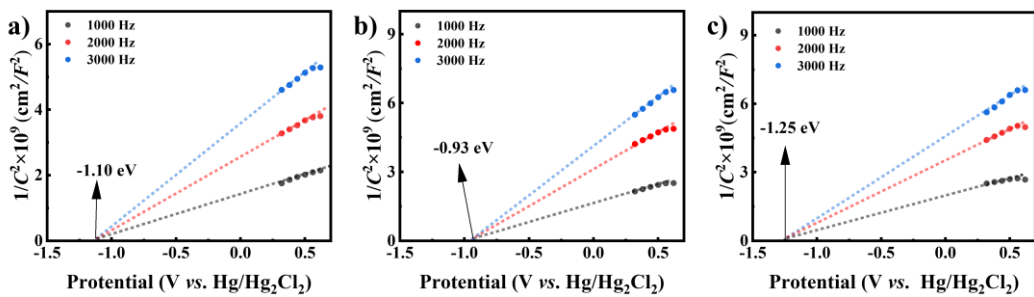


**Figure S8.** Mott-Schottky plots of (a) FCTD-TAPy, (b) FCTD-TAET, and (c) FCTD-TABT

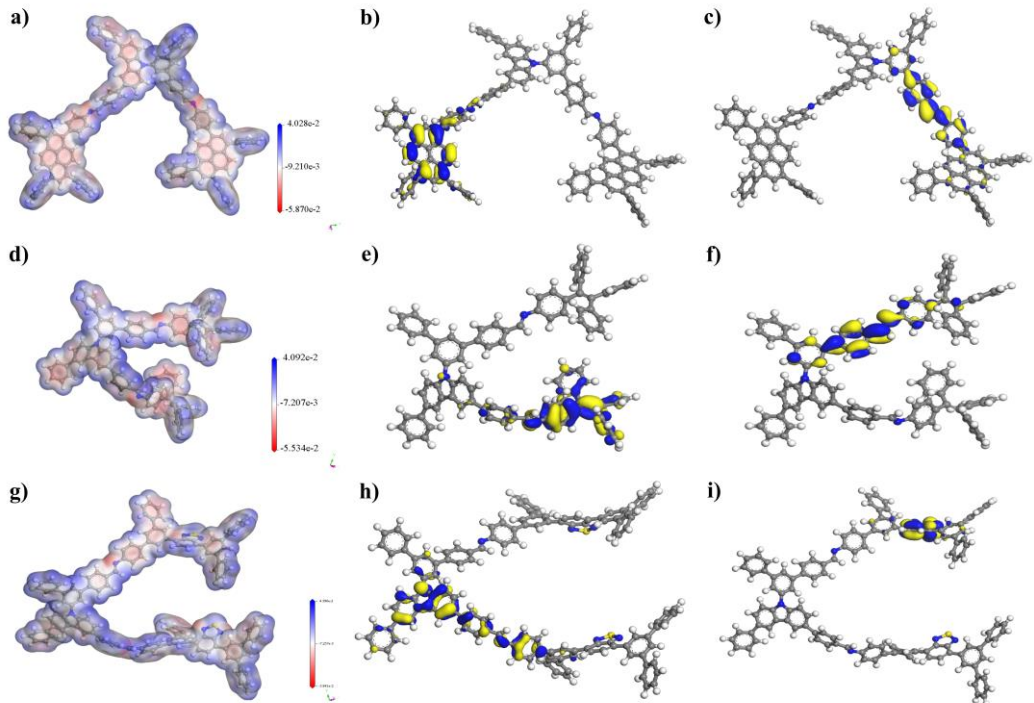


**Figure S9.** (a) Electrostatic potential of FCTD-TAPy simple model, (b) HOMO and (c) LUMO molecular orbital diagrams. (d) Electrostatic potential of FCTD-TAET simple model, (e) HOMO and (f) LUMO molecular orbital diagrams. (g) Electrostatic potential of FCTD-TABT simple model, (h) HOMO and (i) LUMO molecular orbital diagrams.

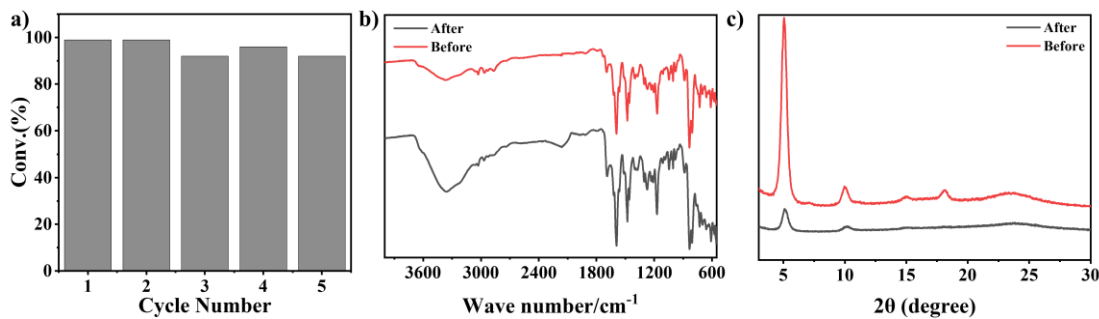


**Figure S10.** (a) Reusability of the FCTD-TAPy, (b) PXRD patterns and (c) FT-IR spectra of FCTD-TAPy after the photocatalytic reaction.

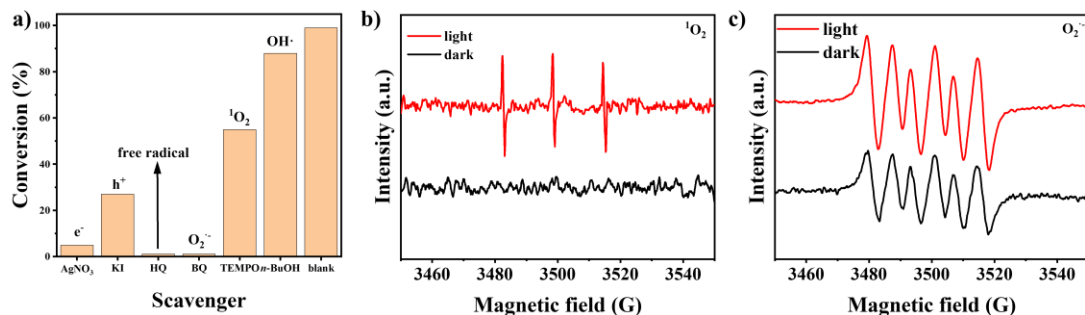


**Figure S11.** (a) Effect of scavengers on the photocatalytic oxidation of benzylamine, (b) in situ EPR signals labeled by TEMPO for <sup>1</sup>O<sub>2</sub> in dispersions and (c) in situ EPR signals labeled by DMPO for O<sub>2</sub><sup>-</sup> in dispersions.

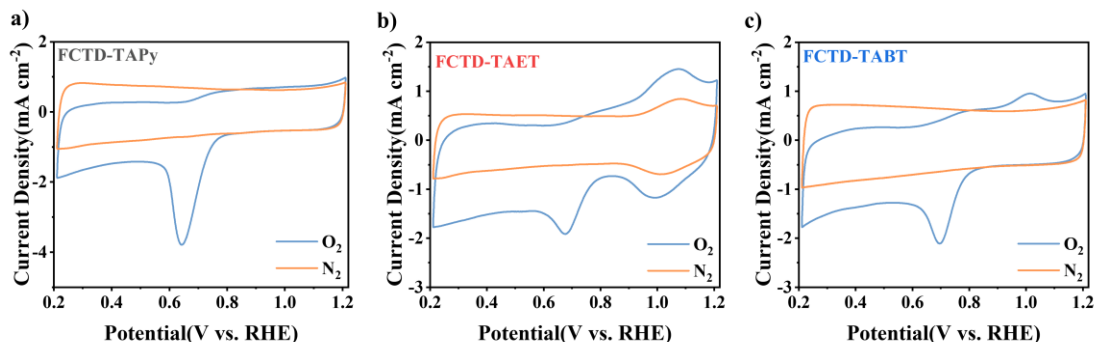
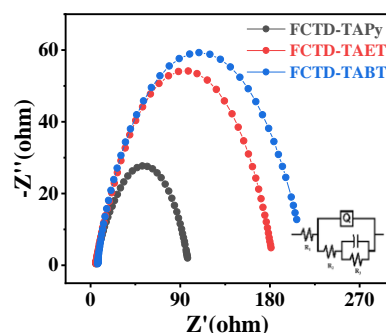


**Figure S12.** CV curves of (a) FCTD-TAPy, (b) FCTD-TAET, and (c) FCTD-TABT at O<sub>2</sub> saturation (blue) and N<sub>2</sub> saturation (orange)



	<b>R</b> <sub>1</sub>	<b>R</b> <sub>2</sub>	<b>R</b> <sub>3</sub>
<b>FCTD-TAPy</b>	5.26	68.97	2.43
<b>FCTD-TAET</b>	5.24	117.3	61.5
<b>FCTD-TABT</b>	6.80	1.60	207.8

**Figure S13.** EIS Nyquist plots of the three COFs

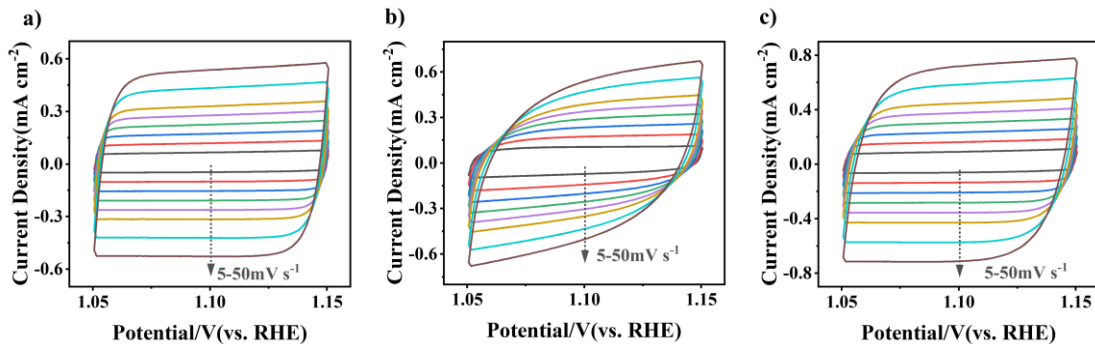


**Figure S14.** CV curves of (a) FCTD-TAPy, (b) FCTD-TAET, and (c) FCTD-TABT at different scanning rates

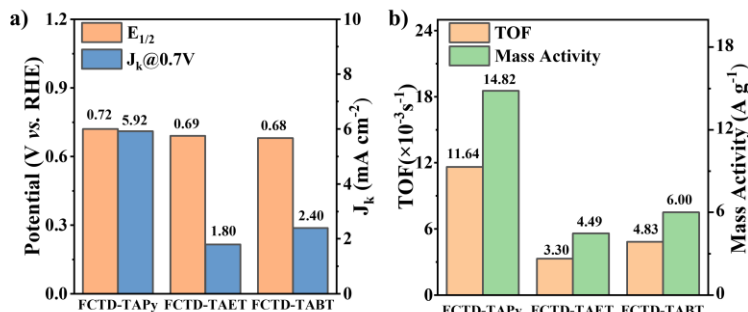


**Figure S15.** (a)  $E_{1/2}$  and  $J_k$  (0.7V vs. RHE) of three COFs in  $O_2$ -saturated 0.1 M KOH, (b) TOFs and mass activities (0.7V vs. RHE) of three COFs in  $O_2$ -saturated 0.1 M KOH.

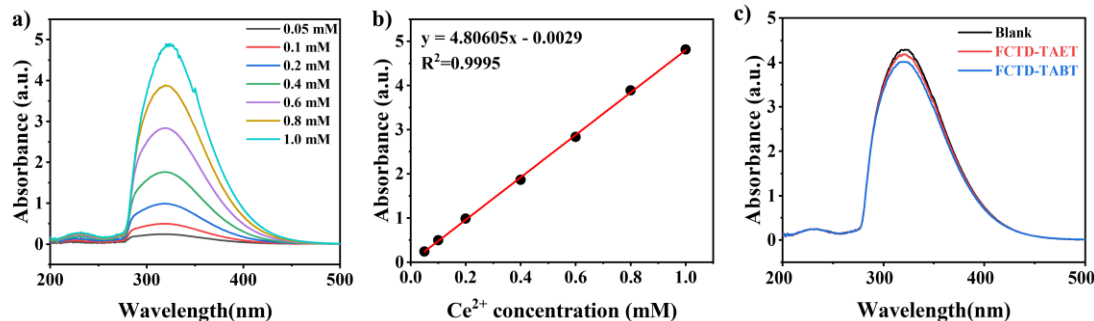


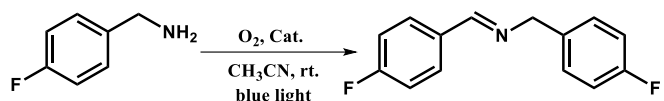
**Figure S16.** UV-visible absorption spectra of Ce<sup>4+</sup> at different concentrations, (b) The relationship between Ce<sup>4+</sup> concentration at 319 nm and absorbance, (c) Effect of electrolyte on Ce<sup>4+</sup> absorbance

after electrocatalytic reaction

**Table S1.** Elemental analyses (C, H and N) for COFs

Sample	Calculated/Found %			Calculated C/N	Found C/N
	C	H	N		
<b>FCTD-TAPy</b>	89.58/88.68	4.34/5.56	6.08/5.76	14.74	15.40
<b>FCTD-TAET</b>	88.34/87.04	4.99/5.76	7.16/7.2	12.34	12.09
<b>FCTD-TABT</b>	85.30/86.47	4.20/6.13	7.92/7.4	10.77	11.69

**Table S2.** Influence of different trapping agents on catalytic effect



Entry	Photocatalyst	Blue light	O <sub>2</sub>	Time(h)	Quencher	Conv. (%)
1	<b>FCTD-TAPy</b>	+	+	12	AgNO <sub>3</sub>	5
2	<b>FCTD-TAPy</b>	+	+	12	KI	27
3	<b>FCTD-TAPy</b>	+	+	12	BQ	<1
4	<b>FCTD-TAPy</b>	+	+	12	TEMPO	55
5	<b>FCTD-TAPy</b>	+	+	12	HQ	<1
6	<b>FCTD-TAPy</b>	+	+	12	n-BuOH	88
7	-	+	+	12	/	17
8	<b>FCTD-TAPy</b>	-	+	12	/	46
9	<b>FCTD-TAPy</b>	+	-	12	/	48

#### 4. Structure simulation data

**Table S3.** Fractional atomic coordinates for simulated **FCTD-TAPy**

Space group: P2
a = 26.740 Å, b = 26.150 Å, c = 5.19468 Å

$\alpha = \gamma = 90.0^\circ$ , $\beta = 118.0^\circ$				
Atom label	Atom type	x	y	z
C1	C	0.02755	1.95224	-2.49217
C2	C	0.05473	1.90502	-2.48356
C3	C	0.05517	1.9993	-2.48565
C4	C	0.10965	1.90478	-2.46151
C5	C	0.13665	1.95136	-2.44873
C6	C	0.11107	1.99904	-2.46076
C7	C	0.14148	1.8566	-2.4407
C8	C	0.1256	1.82482	-2.68465
C9	C	0.15715	1.7807	-2.66676
C10	C	0.20543	1.76768	-2.40686
C11	C	0.2207	1.7991	-2.16049
C12	C	0.18923	1.84328	-2.17842
N13	N	0.23705	1.72234	-2.40148
C14	C	-0.14728	2.04633	-2.58478
C15	C	-0.15018	2.08459	-2.78094
C16	C	-0.18966	2.12426	-2.85932
C17	C	-0.23014	2.12596	-2.76066
C18	C	-0.22763	2.08894	-2.56004
C19	C	-0.18593	2.04996	-2.46917
C20	C	0.97413	1.04496	0.50286
C21	C	1.02676	0.85907	0.50829
C22	C	0.54647	1.33304	-1.48766
C23	C	0.54457	1.2791	-1.51557
C24	C	0.67522	1.17529	-1.94387
N25	N	0.71938	1.15404	-1.94384
C26	C	0.62066	1.57822	-1.7348
C27	C	0.62119	1.66302	-1.92962
C28	C	0.5916	1.62021	-1.90967
C29	C	0.53172	1.45279	-1.58724
C30	C	0.521	1.5033	-1.54964
C31	C	0.5487	1.54454	-1.59803
C32	C	0.58859	1.53479	-1.69645
C33	C	0.59685	1.4837	-1.75899
C34	C	0.56733	1.4427	-1.71267
C35	C	0.71028	1.71277	-1.78569
C36	C	0.68057	1.66559	-1.76898
C37	C	0.68017	1.57992	-1.5805
C38	C	0.70984	1.62341	-1.59505
C39	C	0.66121	1.18828	-1.7084
C40	C	0.64069	1.26651	-1.51128
C41	C	0.67713	1.23707	-1.58059

C42	C	0.58669	1.24801	-1.56902
C43	C	0.60933	1.16856	-1.74627
C44	C	0.57248	1.19788	-1.68281
H45	H	0.17946	1.95007	-2.42018
H46	H	0.08912	1.83459	-2.88908
H47	H	0.14474	1.75686	-2.85747
H48	H	0.25623	1.78935	-1.9531
H49	H	0.20182	1.86701	-1.98681
H50	H	-0.12475	2.08213	-2.8922
H51	H	-0.19296	2.15119	-3.02495
H52	H	-0.25991	2.08826	-2.49022
H53	H	-0.18575	2.02109	-2.31923
H54	H	0.95752	1.08163	0.52119
H55	H	1.04631	0.82243	0.51642
H56	H	0.58415	1.35282	-1.45364
H57	H	0.64427	1.18948	-2.14857
H58	H	0.5975	1.69478	-2.06629
H59	H	0.54583	1.61985	-2.02972
H60	H	0.54074	1.58316	-1.55221
H61	H	0.62491	1.47591	-1.85146
H62	H	0.57088	1.40516	-1.78767
H63	H	0.68558	1.74082	-1.94956
H64	H	0.70343	1.54827	-1.44123
H65	H	0.75557	1.62441	-1.46947
H66	H	0.65465	1.30411	-1.4197
H67	H	0.71546	1.25453	-1.56148
H68	H	0.59431	1.13228	-1.85695
H69	H	0.53191	1.18143	-1.73066
N70	N	0.5	1.4175	0.5
C71	C	0.5	1.36126	0.5
C72	C	0.5	1.25355	0.5

**Table S4.** Fractional atomic coordinates for simulated **FCTD-TAET**

Space group: P2				
$a = 23.040\text{\AA}$ , $b = 22.610\text{\AA}$ , $c = 5.43821\text{\AA}$				
$\alpha = \gamma = 90.0^\circ$ , $\beta = 118.0^\circ$				
Atom label	Atom type	x	y	z
C1	C	0.03079	1.94395	-2.48565
C2	C	0.07	1.88878	-2.42373
C3	C	0.05016	1.84086	-2.60869
C4	C	0.09087	1.79152	-2.55266
C5	C	0.1518	1.78975	-2.31334
C6	C	0.17066	1.83675	-2.12275

C7	C	0.1305	1.88629	-2.1807
N8	N	0.19416	1.74075	-2.27814
C9	C	-0.06339	1.99624	-2.47022
C10	C	-0.07797	2.04791	-2.63182
C11	C	-0.12391	2.08862	-2.6298
C12	C	-0.1551	2.07721	-2.46556
C13	C	-0.13768	2.02758	-2.29623
C14	C	-0.09094	1.9884	-2.29131
C15	C	0.5553	1.32764	-1.46677
C16	C	0.55292	1.26614	-1.49714
C17	C	0.76286	1.15697	-1.62438
N18	N	0.79316	1.11228	-1.46811
C19	C	0.63057	1.59862	-1.79913
C20	C	0.63557	1.69563	-1.97805
C21	C	0.59927	1.65042	-1.9409
C22	C	0.53356	1.46171	-1.59815
C23	C	0.52244	1.52015	-1.55927
C24	C	0.55259	1.5664	-1.62495
C25	C	0.59366	1.55217	-1.74375
C26	C	0.60125	1.49267	-1.80205
C27	C	0.57028	1.44716	-1.73365
C28	C	0.74249	1.74051	-1.87712
C29	C	0.70375	1.68978	-1.86986
C30	C	0.69829	1.59173	-1.70213
C31	C	0.73472	1.63709	-1.73642
C32	C	0.70813	1.18378	-1.59568
C33	C	0.62739	1.26151	-1.7116
C34	C	0.67878	1.23566	-1.74054
C35	C	0.60481	1.23612	-1.53572
C36	C	0.6843	1.15741	-1.42561
C37	C	0.63264	1.18319	-1.39761
H38	H	0.00301	1.84173	-2.79305
H39	H	0.07617	1.755	-2.6981
H40	H	0.21624	1.83562	-1.93059
H41	H	0.14705	1.92312	-2.03757
H42	H	-0.0562	2.05541	-2.76725
H43	H	-0.13626	2.12718	-2.76204
H44	H	-0.16255	2.01874	-2.17391
H45	H	-0.07933	1.94932	-2.16156
H46	H	0.60027	1.35072	-1.42084
H47	H	0.77592	1.17397	-1.77794
H48	H	0.61087	1.73592	-2.08255
H49	H	0.54704	1.65596	-2.02061

H50	H	0.54614	1.61162	-1.57746
H51	H	0.63008	1.48185	-1.90622
H52	H	0.57302	1.40264	-1.79771
H53	H	0.71647	1.77959	-1.98955
H54	H	0.72324	1.5521	-1.59081
H55	H	0.78737	1.63191	-1.65193
H56	H	0.60484	1.30128	-1.82832
H57	H	0.69569	1.2562	-1.87549
H58	H	0.70585	1.11682	-1.31407
H59	H	0.61546	1.16276	-1.26334
N60	N	0.5	1.42247	0.5
C61	C	0.5	1.35905	0.5
C62	C	0.5	1.23492	0.5

**Table S5.** Fractional atomic coordinates for simulated FCTD-TABT

Space group: P2				
$a = 27.4160\text{\AA}$ , $b = 28.1600\text{\AA}$ , $c = 4.4630\text{\AA}$				
$\alpha = \gamma = 90.0^\circ$ , $\beta = 115.0^\circ$				
Atom label	Atom type	x	y	z
C1	C	0.09188	1.9399	-2.69083
C2	C	0.10582	1.89682	-2.7991
C3	C	0.12647	1.97863	-2.64987
C4	C	0.15087	1.89383	-2.87126
C5	C	0.17738	1.93555	-2.88637
C6	C	0.16419	1.9785	-2.78345
C7	C	0.17484	1.84711	-2.88157
C8	C	0.14288	1.80713	-3.0289
C9	C	0.16613	1.76182	-2.97912
C10	C	0.22097	1.75599	-2.77732
C11	C	0.25345	1.79618	-2.65097
C12	C	0.2306	1.84122	-2.70121
N13	N	0.24342	1.70922	-2.70151
C14	C	-0.1882	2.0237	-2.17787
C15	C	-0.1554	2.06417	-2.05888
C16	C	-0.17717	2.10695	-2.01427
C17	C	-0.23195	2.10988	-2.09357
C18	C	-0.26467	2.06957	-2.2061
C19	C	-0.24296	2.02659	-2.24683
C20	C	0.54846	1.35043	-1.40993
C21	C	0.54752	1.30102	-1.43809
C22	C	0.7129	1.17337	-1.38039
N23	N	0.74378	1.15476	-1.09788
C24	C	0.62785	1.57143	-1.6925

C25	C	0.63606	1.65094	-1.87352
C26	C	0.60498	1.61088	-1.89459
C27	C	0.53416	1.45834	-1.57895
C28	C	0.52198	1.50505	-1.54851
C29	C	0.54982	1.54264	-1.60337
C30	C	0.5933	1.53231	-1.68048
C31	C	0.60478	1.4847	-1.72773
C32	C	0.57392	1.44738	-1.68757
C33	C	0.71834	1.6984	-1.58468
C34	C	0.68964	1.65305	-1.63732
C35	C	0.68234	1.5724	-1.46911
C36	C	0.71293	1.61335	-1.43796
C37	C	0.67509	1.21121	-1.40286
C38	C	0.64541	1.27763	-1.17317
C39	C	0.68595	1.2458	-1.1558
C40	C	0.5936	1.27349	-1.43058
C41	C	0.62447	1.20939	-1.66865
C42	C	0.58412	1.23987	-1.68037
C43	C	0.95582	0.94326	0.60312
C44	C	0.97941	0.98651	0.56426
C45	C	1.02153	0.90131	0.4558
N46	N	0.96913	1.03042	0.63292
H47	H	0.08353	1.86469	-2.81965
H48	H	0.12634	2.00904	-2.50542
H49	H	0.20857	1.93425	-2.97472
H50	H	0.09994	1.8107	-3.17305
H51	H	0.14129	1.73094	-3.08441
H52	H	0.29638	1.79258	-2.50698
H53	H	0.25625	1.87119	-2.58252
H54	H	-0.11281	2.06255	-1.99716
H55	H	-0.1521	2.13824	-1.92955
H56	H	-0.30728	2.07215	-2.26947
H57	H	-0.26906	1.99607	-2.33984
H58	H	0.58646	1.36879	-1.32585
H59	H	0.70758	1.15556	-1.60859
H60	H	0.61738	1.68138	-2.02783
H61	H	0.56257	1.61123	-2.05928
H62	H	0.53919	1.57885	-1.57713
H63	H	0.63689	1.4768	-1.8009
H64	H	0.58073	1.41159	-1.74675
H65	H	0.70365	1.72438	-1.78269
H66	H	0.70008	1.54263	-1.30532
H67	H	0.75417	1.61474	-1.25265

H68	H	0.65335	1.30312	-0.97627
H69	H	0.72504	1.24708	-0.94706
H70	H	0.61547	1.18313	-1.86242
H71	H	0.54496	1.23654	-1.88316
H72	H	1.03692	0.86677	0.44015
S73	S	1	1.07692	0.5
N74	N	0.5	1.42671	0.5
C75	C	0.5	1.37572	0.5
C76	C	0.5	1.27685	0.5

## 5. Others

**Table S6.** Different COFs performance for electrocatalytic ORR

Materials	$E_o$ (V)	$E_{1/2}$ (V)	Tafel slope (mV/dec)	$C_{dl}$ (mF cm <sup>-2</sup> )	Ref
FCTD-TAPy	0.84	0.72	51.07	10.56	
FCTD-TAET	0.84	0.69	66.55	9.51	This work
FCTD-TABT	0.87	0.68	53.01	14.26	
JUC-616	/	0.78	52.91	8.62	[1]
CoPc-2SO <sub>3</sub> H-COF	0.82	/	63.2	0.15	[2]
COF-112Co	0.87	0.76	74.32	9.11	[3]
CoF/NG	0.91	0.80	78	9.66	[4]
Py-TD-COF	0.834	0.698	252	/	[5]
Py-TD-COF-NH	0.829	0.693	281	/	
PTh-COF/CNT	/	0.75	45.7	8.6	[6]
PYTA-PB-COF	0.88	0.78	67.9	7.9	[7]

CoPc-EA-COF	0.901	0.803	128	16.2	[8]
CoNP-s-IMCOF	/	0.83	107	0.031	[9]
CoTAPP-PATA-COF	0.926	0.801	55	10.64	[10]

**Table S7.** Comparisons of different photocatalysts for the selective oxidation of benzylamine

Photocatalyst	Conditions	Conv. (%)	Sel. (%)	Ref
COF-TpPa (10 mg)	Benzylamine (0.9 mmol), O <sub>2</sub> (1 atm), CH <sub>3</sub> CN (6 mL), 5.0 W 420 nm LED, and 5.0 h	78	99	[11]
ToAzo-COF (5 mg)	Benzylamine (0.3 mmol), Air, CH <sub>3</sub> CN (1 mL), rt., 3.0 W × 4 460 nm LED, and 1.8 h	90	99	[12]
BTT-Bpy-COF (10 mg)	Benzylamine (0.5 mmol), O <sub>2</sub> (1 atm), CH <sub>3</sub> CN (3 mL), rt., 5.0 W × 4 465 nm LED, and 3 h	99	99	[13]
W18O49@TpPa-H-0,1 (10 mg)	Benzylamine (0.1 mmol), Air , CH <sub>3</sub> CN (5 mL), rt., 10.0 W 420-425 nm LED, and 2 h	99	99	[14]
UiO-66- NH <sub>2</sub> @Au <sub>0.5</sub> @COF1 (20 mg)	Benzylamine (1 mmol), O <sub>2</sub> (1 atm), CH <sub>3</sub> CN (3 mL), 420 nm light, and 20 h	66.9	96.9	[15]
COF-NUST-36 (4 mg)	Benzylamine (0.1 mmol), O <sub>2</sub> (1 atm), CH <sub>3</sub> CN (1.5 mL), rt., 30.0 W 455-460 nm light, and 2.5 h	97	95	[16]
PY-BT COF (5 mg)	Benzylamine (0.1 mmol), O <sub>2</sub> (1 atm), CH <sub>3</sub> CN (2 mL), rt., 300 W 455-460 nm light, and 2.5 h	99	/	[17]
FCTD-TAPy (5 mg)	4-Methylbenzylamine (0.1 mmol), O <sub>2</sub> (1 atm), CH <sub>3</sub> CN (2 mL), rt., 30 W 450-460 nm light, and 12 h	95	99	This work

## 6. References

1. J. Li, J. Jia, J. Suo, C. Li, Z. Wang, H. Li, V. Valtchev, S. Qiu, X. Liu, Q. Fang. *Journal of Materials Chemistry A*, 2023, **11**, 18349.
2. R. Jiang, Q. Zhi, B. Han, N. Li, K. Wang, D. Qi, W. Li, J. Jiang. *Chemical Engineering Journal*, 2024, **489**, 151232.
3. J. Li, P. Liu, J. Mao, J. Yan, W. Song. *Nanoscale*, 2022, **14**, 6126.
4. Y. Shin, S. Park, H. Jang, G. Shin, D. Shin, S. Park. *Nanoscale*, 2024.
5. S. Huang, B. Zhang, D. Wu, Y. Xu, H. Hu, F. Duan, H. Zhu, M. Du, S. Lu. *Applied Catalysis B: Environmental*, 2024, **340**, 123216.
6. Z. Chen, P. Fang, X. Zou, Z. Shi, J. Zhang, Z. Sun, S. Guo, F. Yan. *Small*, 2024, 2401880.
7. X. Yang, Y. Fu, M. Liu, S. Zheng, X. Li, Q. Xu, G. Zeng. *Angewandte Chemie International Edition*, 2024, **63**, e202319247.
8. M. Liu, S. Yang, Y. Fu, X. Yang, X. Li, J. He, Q. Xu, G. Zeng. *Chemical Engineering Journal*, 2024, **488**, 150812.
9. J.-M. Ju, C. H. Lee, J. H. Park, J.-H. Lee, H. Lee, J.-H. Shin, S.-Y. Kwak, S. U. Lee, J.-H. Kim. *ACS applied materials & interfaces*, 2022, **14**, 24404.
10. M. Liu, S. Liu, C. X. Cui, Q. Miao, Y. He, X. Li, Q. Xu, G. Zeng. *Angewandte Chemie*, 2022, **134**, e202213522.
11. Z. Wu, X. Huang, X. Li, G. Hai, B. Li, G. Wang. *Science China Chemistry*, 2021, **64**, 2169.
12. K. Xiong, Y. Wang, F. Huang, K. Zhang, B. Zeng, X. Lang. *Journal of Colloid and Interface Science*, 2024, **665**, 252.
13. J. Kou, G. Wang, H. Guo, L. Li, J. Fang, J. Ma, Z. Dong. *Applied Catalysis B: Environment and Energy*, 2024, **352**, 124020.
14. X. Zhao, A. Li, D. Yang, T.-Y. Qiu, Z. Zhao, S.-L. Wang, X. Mu, H.-Q. Tan. *Journal of Colloid and Interface Science*, 2024, **653**, 67.
15. K. Zhang, Z. Xi, Z. Wu, G. Lu, X. Huang. *ACS Sustainable Chemistry & Engineering*, 2021, **9**, 12623.
16. Z. Gu, Z. Shan, Y. Wang, J. Wang, T. Liu, X. Li, Z. Yu, J. Su, G. Zhang. *Chinese Chemical Letters*, 2024, **35**, 108356.
17. M.-Y. Yang, S.-B. Zhang, M. Zhang, Z.-H. Li, Y.-F. Liu, X. Liao, M. Lu, S.-L. Li, Y.-Q. Lan. *Journal of the American Chemical Society*, 2024, **146**, 3396.